LIMNOLOGY
and
OCEANOGRAPHY

ASLO

Limnol. Oceanogr. 00, 2015, 00–00

doi: 10.1002/lno.10130

Biogeochemical and metagenomic analysis of nitrite accumulation in the Gulf of Mexico hypoxic zone

Laura A. Bristow,[1] Neha Sarode,[2] John Cartee,[2] Alejandro Caro-Quintero,[2] Bo Thamdrup,[1] Frank J. Stewart*[2]

[1]Department of Biology and Nordic Center for Earth Evolution (NordCEE), University of Southern Denmark, Odense, Denmark

[2]School of Biology, Georgia Institute of Technology, Ford ES&T Building, Rm 1242, 311 Ferst Drive, Atlanta, Georgia

Abstract

The Louisiana Shelf in the Gulf of Mexico experiences recurrent bottom water hypoxia under summertime eutrophic conditions. The onset, maintenance, and breakdown of hypoxia are associated with dynamic microbial biogeochemical cycles. However, the distribution of microbial taxa and metabolisms across Shelf oxygen gradients remains under-characterized. We combined biogeochemical analyses of nitrogen (N) distributions and metabolic rates with metagenomic and metatranscriptomic analysis of summertime Shelf waters. Samples from an east–west transect during July 2012 revealed an inverse relationship between nitrite and oxygen concentrations, with concentrations exceeding 1 μmol L^{-1} at $\sim$ 50% oxygen saturation and reaching 4.6 μmol L^{-1} at the most oxygen-depleted sites. Historical data confirms that nitrite accumulation occurs frequently in this region both above and below the hypoxic threshold. Experimental incubations demonstrated a strong decoupling between the two steps of nitrification, with ammonia oxidation proceeding up to 30 times faster than nitrite oxidation under low oxygen. 16S rRNA gene, metagenome, and metatranscriptome sequencing revealed a diverse microbial community, stratified over shallow ($<$ 10 m) depth gradients, with an enrichment of ammonia-oxidizing Thaumarchaeota genes and transcripts in deeper more oxygen-depleted layers, and a comparatively low representation of sequences related to nitrite oxidation. A range of factors, including temperature and substrate availability, which may be linked indirectly to bottom water oxygen content, potentially drives decoupling of ammonia and nitrite oxidation on the Louisiana Shelf. Nitrite accumulation in hypoxic zones remains understudied and may have important effects on microbial nitrogen flux, algal dynamics, and production.

Oxygen concentration is a fundamental driver of microbial metabolism and biogeochemical cycling in aquatic ecosystems. In coastal ecosystems, such as the shallow waters of the Louisiana Shelf in the northern Gulf of Mexico (GoM), oxygen concentrations vary substantially over seasonal and spatial gradients (Turner et al. 2008). Shelf oxygen gradients are associated with variations and fluxes of key bioactive substrates, including organic carbon, and macronutrients and micronutrients, the dynamics of which have been well characterized as part of a comprehensive long-term monitoring program (Rabalais et al. 2002; Turner et al. 2007). In contrast, the microorganisms regulating material and energy cycling in the pelagic Shelf ecosystem remain undercharacterized. Oxygen is a primary determinant of the taxonomic composition of Shelf microbial communities (King et al. 2013; Tolar et al. 2013). However, it remains unclear how changes in microbial abundance or activity affect processes such as nitrification or denitrification, which involve interdependent metabolic transformations by different microbial guilds. Varied responses of microbial taxa to oxygen depletion may decouple important steps in elemental cycles, thereby influencing bulk fluxes, as well as standing stocks of bioavailable intermediates such as nitrite. The accumulation of nitrite may affect the pathways of microbial nitrogen cycling, as nitrite is a pivotal intermediate in microbial N transformations (Thamdrup et al. 2012). Accumulation may also influence phytoplankton dynamics, given that the kinetics of nitrite utilization vary greatly between different algal species (Collos 1998; Malerba et al. 2012).

Additional Supporting Information may be found in the online version of this article.

Conflict of Interest: The authors have no competing commercial interests in relation to this work.

Laura A. Bristow and Neha Sarode contributed equally to this work.

*Correspondence: frank.stewart@biology.gatech.edu

Episodically occurring patches of low oxygen water are common features of Louisiana Shelf waters with important implications for ecosystem structuring (Diaz and Rosenberg 2008; Rabalais et al. 2010; Zhang et al. 2010). Hypoxia occurs where microbial respiration of organic biomass depletes oxygen concentrations to below 2 mg L^{-1} ($\sim$ 63 μmol kg^{-1}). Louisiana Shelf hypoxia typically encompasses 20% to 50% of the total water column during summer (Rabalais et al. 2001) when nutrients from the Mississippi and Atchafalaya rivers fuel high levels of primary production. Although Shelf hypoxia can form naturally, enhanced riverine nutrient influx due to human activities has increased the intensity and extent of hypoxic layers in the northern GoM and throughout the world's oceans over the last half-century (Diaz and Rosenberg 2008; Rabalais et al. 2010). In years of high nutrient runoff, the GoM hypoxic zone is one of the largest in the world (Rabalais et al. 2002, 2007; Bianchi et al. 2010), extending over an area of up to 22,000 km^2. In other years, including at the time of this study in 2012 when drought in the upper U.S.A led to decreased river outflow, the spatial extent of hypoxia is far less. However, dynamic oxygen and nutrient gradients occur on the Shelf in all years, as documented by LUMCON (Louisiana Universities Marine Consortium) monitoring over the past 30 yr (Turner et al. 2006, 2012). The internal turnover of nutrients and its potential linkage to Shelf hypoxia have been studied only rarely (Dagg et al. 2007).

Nitrification plays a key role in aquatic systems, linking the most oxidized and most reduced species of the N cycle. The process involves a two-step conversion of ammonium to nitrate (via nitrite), carried out by phylogenetically distinct groups of organisms, namely ammonia-oxidizing archaea (AOA), ammonia-oxidizing bacteria (AOB), and nitrite-oxidizing bacteria (NOB). Nitrification is, thus, a key step in the regeneration of nitrate, which supports phytoplankton growth in the sunlit ocean, as well as N loss through denitrification under functionally anoxic conditions. The first step of nitrification (ammonia oxidation to nitrite) is mediated by both AOB and AOA (Francis et al. 2005; Mosier and Francis 2008). Under low oxygen conditions, marine ammonia oxidation appears to be conducted primarily by AOA in the phylum Thaumarchaeota (Lam et al. 2009; Beman et al. 2012; Stewart et al. 2012). The second step of nitrification (nitrite oxidation to nitrate) is carried out by NOB, notably the marine genera *Nitrospina* and *Nitrospira*. These clades are adapted for microaerophilic metabolism (Lücker et al. 2010, 2013), remaining efficient at nitrite consumption even at the nanomolar oxygen concentrations typical of OMZ boundaries (Füssel et al. 2012; Beman et al. 2013).

In many aquatic environments, including sediments (Meyer et al. 2005), wastewater treatment systems (Schramm et al. 1999), and most marine waters (Ward 2008), the two steps of nitrification are tightly coupled such that nitrite does not accumulate to any appreciable extent. However, nitrite accumulation is observed consistently in some environments. The most extensive accumulation of nitrite occurs in the functionally anoxic core of oceanic oxygen minimum zones (OMZs) where oxygen concentrations fall below 0.1 μmol kg^{-1} and dissimilatory nitrate reduction generates 1–10 μmol L^{-1} nitrite (Thamdrup et al. 2012; De Brabandere et al. 2014), while nitrite oxidation is limited by oxygen availability (Cline and Richards 1972).

Nitrite accumulation may also occur in environments where oxygen is not limiting, presumably due to a decoupling of ammonia and nitrite oxidation. Periodic accumulations of nitrite associated with Thaumarchaeota ammonia-oxidizer blooms have been observed across diverse coastal ecosystems (Pitcher et al. 2011; Hollibaugh et al. 2014). In estuaries, a nitrite maximum can be found at intermediate salinities, where high rates of ammonia oxidation may generate >10 μmol L^{-1} nitrite while growth and activity of NOB are apparently limited by changing salinity combined with short hydraulic retention times (Billen 1975; McCarthy et al. 1984). Likewise, uncoupling of ammonia and nitrite oxidation represents one potential explanation for the formation of the "primary nitrite maximum" of 0.1–0.5 μmol L^{-1} observed at the base of the photic zone in some oceanic settings (Brandhorst 1958; Lomas and Lipschultz 2006; Beman et al. 2013; Santoro et al. 2013). However, the potential drivers of uncoupling are best understood for artificial systems, for example in biological wastewater treatment where inhibition of nitrite oxidation is achieved in part through temperature ($>$ 25°C) limitation of NOB, or by a combination of high, inhibitory ammonia concentrations and low oxygen ($<$ 10 μmol kg^{-1}) (Schmidt et al. 2003; Van Hulle et al. 2010). In natural systems, an effect of temperature has not been observed (Ward 2008), ammonia typically does not reach inhibitory levels (Van Hulle et al. 2010), and other potential controls on nitrification steps (e.g., photoinhibition) (Olson 1981) remain poorly constrained (Bouskill et al. 2011).

To date only a single profile of nitrification rates has been described for the hypoxic GoM, with observed rates up to 3.5 μmol L^{-1} d^{-1} (Carini et al. 2010). In that study, ammonia and nitrite oxidation rates were not determined independently, so the extent of coupling could not be resolved. Hence, the spatial distribution and drivers of this environmentally important two-step process, notably in relationship to the strong physiochemical gradients observed in the hypoxic GoM, remain poorly characterized.

Only a handful of studies have characterized the microbial taxonomic composition of northern GoM waters (King et al. 2013; Tolar et al. 2013). King et al. (2013) quantified bacterioplankton 16S rRNA gene diversity within both the Mississippi River water outflow plume and on- and off-shelf sites in the northern GoM. This work concluded that prior to the development of hypoxia, community composition varied substantially with depth but diversity indices showed no considerable variation over biological and

physiochemical gradients, indicating a relatively stable bacterioplankton community structure. Both King et al. (2013) and Tolar et al. (2013) reported vertical stratification of Thaumarchaeota subclades and a general trend of increased Thaumarchaeota abundance with depth. Interestingly, Tolar et al. (2013) also identified a diverse community of Thaumarchaeota (up to 40% of prokaryotes), unique to the northern GoM, with subpopulations segregated by depth (near-surface $\leq$ 100 m and deep $>$ 100 m). At the time of their sampling prior to the onset of summer hypoxia, Thaumarchaeota were 20-fold more abundant than NOB. However, the relative abundances of these groups were correlated ($r^2 = 0.5$), which was interpreted as evidence for a tight coupling between the two steps of nitrification and, therefore, an efficient conversion of ammonium to nitrate. Nitrification rate measurements, however, were not reported, nor were the relative expression levels of key functional genes mediating N cycling in this region.

Given the comparatively high oxygen concentrations of the GoM water column relative to anoxic OMZs where nitrate reduction dominates and given prior evidence of ammonia and nitrite oxidizer coupling in this system, we hypothesized that nitrification on the Louisiana Shelf proceeds efficiently with limited nitrite accumulation. We test this hypothesis by combining biogeochemical analyses of N cycling with the first metagenome and metatranscriptome data from Louisiana Shelf microbial communities. These analyses identify a diverse and stratified community whose metabolic properties and biochemical activities appear linked to an unexpected accumulation of nitrite in hypoxic zone-associated waters, suggesting a decoupling of key N cycle processes. We then explore potential drivers of this decoupling.

Methods

Sampling

Samples for biogeochemical and microbial molecular analysis were collected from eight stations on the Louisiana Shelf during a research cruise aboard the R/*V Cape Hatteras* (23 July 2012 to 3 August 2012). Seawater was sampled from depths spanning oxygenated surface waters to low oxygen bottom waters above the sediment–water interface (Fig. 1; Supporting Information Table S1). Collections were made using Niskin bottles deployed on a rosette containing a Conductivity–Temperature-Depth profiler (SBE 911plus) equipped with a WetLabs fluorometer and SBE43 dissolved oxygen sensor. The steepest oxygen gradient between surface and bottom waters was observed at Sta. 6 (Fig. 1). We therefore targeted this station for high-resolution (every 2 m; 31st July) vertical sampling for metagenomics (DNA). Samples for metatranscriptomics (RNA) were collected for three depths (3 m, 9 m, and 13 m) during high-resolution sampling at Sta. 6 (Supporting Information Table S1). We also targeted Sta. 6 for a day-night (diel) survey, during which seawater was collected at two depths (7 m and 15 m) approximately every 4 h over a 57-h period (July 29–31).

Biogeochemical analysis

Nitrite concentrations were determined onboard immediately after collection using the Griess method (Grasshoff et al. 1983). Samples for nitrate and ammonium analysis were filtered through glass fiber filters (GF/F; pore size 0.7 μm) into acid cleaned HDPE bottles and frozen until analysis. Nitrate + nitrite concentrations were determined using chemiluminescence after reduction to nitric oxide with acidic vanadium (III) (Braman and Hendrix 1989). Ammonium concentrations were analyzed fluorometrically with the orthophthaldialdehyde method (Holmes et al. 1999), with a detection limit of 20 nmol L^{-1}.

Rate measurements

Rate determination experiments were carried out at two to three depths per station to capture gradients in oxygen and nitrite (Supporting Information Table S1). Water was sampled directly from the Niskin bottle into 120 mL serum bottles, allowing water to overflow for approximately three volume changes before sealing (without bubbles) with deoxygenated butyl rubber stoppers (De Brabandere et al. 2012). Bottles were stored in the dark at in situ temperature until the start of the experiment (always $<$ 6 h). Serum bottles were amended with ^{15}N labeled substrates. Two ^{15}N amendments were carried out at all stations and depths: addition of 1 μmol L^{-1} $^{15}NH_4^+$ + 1 μmol L^{-1} $^{14}NO_2^-$ to measure ammonia oxidation, and addition of 1 μmol L^{-1} $^{15}NO_2^-$ + 2 μmol L^{-1} $^{14}NO_3^-$ to measure nitrite oxidation. In a third amendment, 2 μmol L^{-1} $^{15}NO_3^-$ + 1 μmol L^{-1} $^{14}NO_2^-$ was added to bottom water from Sta. 4 and Sta. 6 to measure dissimilatory nitrate reduction to nitrite. For each amendment, four serum bottles were spiked with ^{15}N substrate. Saturated $HgCl_2$ (200 μL) was immediately added to one bottle, which served as a killed control. A volume of 20 mL was subsequently removed from all bottles to create a headspace, which was then flushed twice with helium. The removed 20 mL was filtered through a 0.22 μm cellulose acetate filter and frozen for time zero analysis. Injections of air or pure oxygen were then made into the headspace to match in situ oxygen concentrations (determined from the SBE43) with oxygen solubility determined from García and Gordon (1992). A subset of the amendments with labeled nitrate received no oxygen injection and, therefore, represented anoxic conditions. After 12 h and 24 h, an additional 20 mL was removed, filtered, and frozen. After removing the sample at 12 h, headspaces were flushed twice with helium and oxygen additions were made again. After 24 h, oxygen concentrations in the serum bottles were determined using a PreSense oxygen sensor and were always within 12% of observed in situ concentration (from the SBE43). In the anoxic incubations with labeled nitrate, oxygen concentrations were always below 0.7 μmol kg^{-1}.

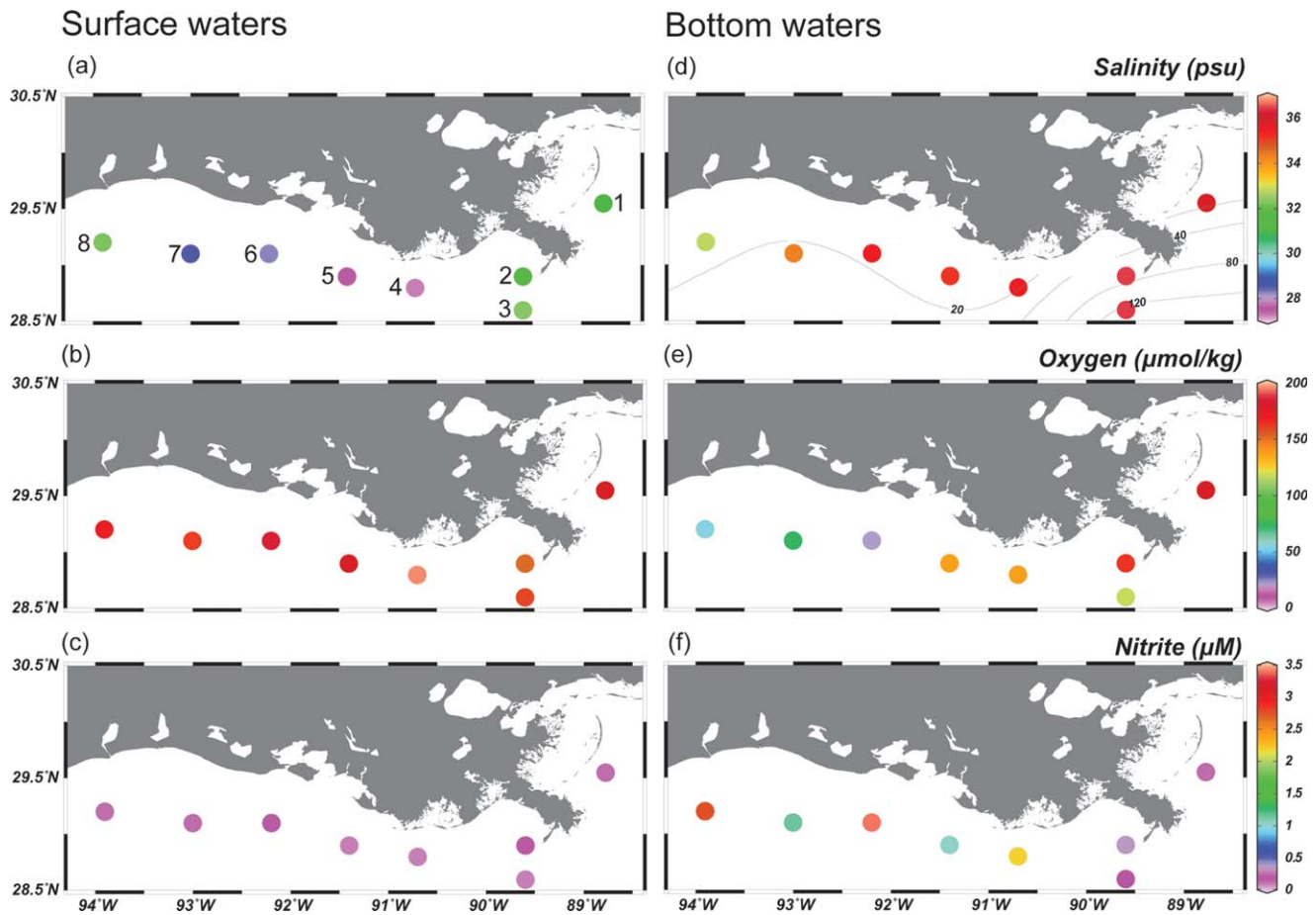

Fig. 1. Salinity (top, a and d), oxygen (μmol kg^{-1}; middle, b and e) and nitrite (μmol L^{-1}; bottom, c and f) distribution throughout the sampling region, in surface and bottom waters (left and right columns, respectively). The station numbers are noted in (a), while the bottom depths are represented as contour lines in (d).

Nitrite oxidation rates were determined based on $^{15}NO_3^-$ production in incubations with $^{15}NO_2^-$. After removal of any unused $^{15}NO_2^-$ from the initial amendment using sulfamic acid, $^{15}NO_3^-$ was converted to $^{15}NO_2^-$ with cadmium and then to N_2 with sulfamic acid (McIlvin and Altabet 2005; Füssel et al. 2012). Ammonia oxidation and nitrate reduction rates were determined based on $^{15}NO_2^-$ production in incubations with $^{15}NH_4^+$ or $^{15}NO_3^-$. $^{15}NO_2^-$ produced during incubations was converted to N_2 with sulfamic acid, following Füssel et al. (2012). The N_2 produced ($^{14}N^{15}N$ and $^{15}N^{15}N$) was analyzed on a gas-chromatography isotope ratio mass spectrometer (GC-IRMS) as in Dalsgaard et al. (2012). Rates for all processes were evaluated from the slope of the linear regression of ^{15}N production with time and corrected for the fraction of the N pool labeled in the initial substrate pool. A *t*-test was applied to determine if rates were significantly different from zero ($p < 0.05$). Nonsignificant rates are presented as not detected.

Recent studies establish the importance of applying a kinetic correction to account for the effect of substrate addition on ammonia oxidation measurements (Horak et al. 2013). Using the equation and K_m of Horak et al. (2013) results in a decrease of our ammonia oxidation rates by 6% to 13%. A study conducted near Sta. 4 measured ammonium regeneration at < 0.05 μmol L^{-1} h^{-1} (Gardner et al. 2009). It is possible that regeneration (not measured) also occurred in our incubations, which could result in underestimation of ammonia oxidation rates. Due to these two counteracting factors (kinetics, ammonium regeneration), no corrections were applied to our rate calculations.

Molecular analysis

Nucleic acid collection and extraction

Microorganisms were collected for DNA and RNA analysis by sequential in-line filtration of seawater (10 L) through a glass fiber disc prefilter (GF/A, 1.6 μm pore-size, 47mm dia., Whatman) and a primary collection filter (Sterivex^{TM}, 0.22 μm pore-size, Millipore) using a peristaltic pump. Biomass on Sterivex filters was used for molecular analysis. These filters were filled with either lysis buffer ($\sim$ 1.8 mL; 50 mmol L^{-1}

Tris-HCl, 40 mmol L^{-1} EDTA, and 0.73 mol L^{-1} sucrose) for DNA samples or RNA stabilization buffer (25 mmol L^{-1} sodium citrate, 10 mmol L^{-1} EDTA, 70 g ammonium sulfate/100 mL solution, pH 5.2) for RNA samples, capped at both ends, and flash-frozen (RNA samples only). Filters were stored at −80°C until extraction. For RNA samples, less than 20 min elapsed between sample collection (water on deck) and fixation in RNA stabilization buffer. We filtered for DNA following filtration for RNA, using the same water sample.

Community DNA was extracted from Sterivex filters using a phenol:chloroform protocol. Cells were lysed by adding lysozyme (2 mg in 40 μL of lysis buffer per filter) directly to the Sterivex cartridge, sealing the caps/ends, and incubating for 45 min at 37°C. Proteinase K (1 mg in 100 μL lysis buffer, with 100 μL 20% SDS) was added, and the cartridges were resealed and incubated for 2 hours at 55°C. The lysate was removed, and nucleic acids were extracted with phenol:-chloroform:isoamyl alcohol (25: 24: 1) and again with chloroform:isoamyl alcohol (24: 1). The aqueous phase was concentrated by spin dialysis through Amicon Ultra-4 w/100 kDa MWCO centrifugal filters.

Community RNA was extracted from Sterivex filters using the *mir*Vana™ miRNA Isolation kit (Ambion). Sterivex filters were thawed on ice, and the RNA stabilization buffer in each cartridge was expelled via syringe and discarded. Cells were lysed by adding Lysis buffer and miRNA Homogenate Additive (Ambion) directly into the cartridge. Following vortexing and incubation on ice, the lysate was expelled into RNAse-free microcentrifuge tubes via syringe and processed using an acid-phenol:chloroform extraction according to the kit protocol. The RNA extract was incubated with TURBO DNA-free™ to remove DNA, and purified and concentrated using the RNeasy MinElute Cleanup kit (Qiagen).

16S rRNA gene PCR and amplicon sequencing

Illumina sequencing of dual-indexed PCR amplicons spanning the V4 region of the 16S rRNA gene was used to assess prokaryote community composition. Amplicons were synthesized using Platinum® PCR SuperMix (Life Technologies) with primers F515 and R806 (Caporaso et al. 2010). Both forward and reverse primers were barcoded and appended with Illumina-specific adapters as in Kozich et al. (2013). Thermal cycling conditions were: initial denaturation at 94°C (3 min), followed by 30 cycles of denaturation at 94°C (45 s), primer annealing at 55°C (45 s) and primer extension at 72°C (90 s), followed by final extension at 72°C for 10 min. Amplicons were analyzed by agarose gel electrophoresis to verify size (~ 400 bp) and purified using the Diffinity RapidTip® for PCR Purification. Amplicons from each sample were pooled at equimolar concentrations and used for paired end (250 × 250 bp) sequencing on an Illumina MiSeq with 5% PhiX genomic library control.

Metagenome and metatranscriptome preparation and sequencing

Shotgun sequencing of community DNA (metagenome) and cDNA (metatranscriptome) was used to analyze functional gene content and transcription in a subset of samples (Supporting Information Table S1). Barcoded DNA libraries were prepared using the Nextera XT DNA sample preparation kit (Illumina). Barcoded cDNA libraries were prepared using the ScriptSeq™ v2 RNA-Seq library preparation kit (Epicenter), with fragment size assessed using an Agilent 2100 Bioanalyzer. DNA and cDNA libraries were used as template for paired end (250 × 250 bp) sequencing on an Illumina MiSeq (Supporting Information Table S2).

Sequence analysis—16S rRNA gene amplicons

Demultiplexed amplicon read pairs were quality trimmed with Trim Galore (Babraham Bioinformatics), using a base Phred33 score threshold of Q25 and a minimum length cutoff of 100 bp. Paired reads were merged using the software FLASH (Magoc and Salzberg 2011) and merged reads analyzed using the software pipeline QIIME v1.8.0 (Caporaso et al. 2010). Sequences were clustered into Operational Taxonomic Units (OTUs) at 97% sequence similarity in QIIME using an open-reference OTU picking protocol with the script pick_open_reference_otus.py. Taxonomy was assigned to a representative OTU per cluster using the Greengenes database (Aug 2013 release). Diversity analysis was performed using the workflow script core_diversity_analyses.py at an even sampling depth ($n = 661$). Relationships between environmental factors and community composition were assessed by environmental factor fitting and nonmetric multidimensional scaling (NMDS) analysis using Vegan version 2.2-1 (Okasen et al. 2007).

Sequence analysis—metagenomes and metatranscriptomes

Analysis of unassembled protein-coding genes and transcripts followed that of Ganesh et al. (2014). Illumina reads were quality trimmed using the FASTX toolkit with a quality score and minimum length cutoff of Q25 and 100 bp, respectively. Custom perl scripts utilizing the USEARCH algorithm (Edgar 2010) were used to merge paired reads with minimum 10% overlap and 95% nucleotide identity within the overlapping region. rRNA transcripts within the quality-processed and merged metatranscriptome reads were identified using riboPicker (Schmieder et al. 2012) and discarded.

Preprocessed metagenome and metatranscriptome sequences were queried against the NCBI-nr database (as of March 2014) using RAPSearch2 (Zhao et al. 2012). Sequences with matches to prokaryote genes (Bacteria or Archaea) above bit score 50 were retained for analysis. The proportional abundance of a gene was calculated as a percentage of the total number of reads matching NCBI-nr. Sequences matching genes for ammonia monooxygenase (*amoC*), nitrite oxidoreductase (*nxrB*), and nitrate reductase (*narG*) were extracted by parsing RAPSearch2 output via keyword queries based on

NCBI-nr annotations, as in Ganesh et al. (2014). Genbank annotations of matched genes were examined manually and via BLASTX to confirm gene identity.

Protein-coding genes and transcripts were classified into KEGG functional categories. Briefly, NCBI GI and RefSeq numbers were parsed from RAPSearch2 output (against NCBI-nr) using custom scripts. These identifiers were used to retrieve corresponding unique md5id's using the md5nr Genbank.md5id2func and RefSeq.md52id2func files. The md5id was then assigned to a KEGG category using the md5nr KEGG.md5id2ont mapping file. Abundance per category was calculated as a proportion of the total number of reads mapping to the KEGG orthology. The taxonomic identity of sequences was determined using custom scripts. Briefly, scientific names associated with NCBI-nr genes identified by RAPSearch2 were used to extract taxonomic identifiers (taxid's) and to assign a full taxonomic lineage, using the names.dmp and nodes.dmp files from NCBI.

KEGG categories differing in proportional abundance between surface (< 10 m; $n = 13$) versus mid-deep (≥10 m; $n = 10$) metagenomes were detected using Gene Set Enrichment Analysis (GSEA) implemented in CLC Genomics workbench 8.0, according to Tian et al. (2005). Samples from each depth category were treated as replicates (biological replicates per depth were not available). Raw mapped read counts were used as input, with the counts then normalized using the 'By totals' option with default settings. Categories with less than 10 mapped genes were excluded. p values were calculated over 10,000 permutations, with a false detection rate (FDR) correction obtained using R stats function p adjust (http://www.R-project.org/) by the method of Benjamini and Hochberg (1995).

Sequence counts are provided in Supporting Information Table S2 and all sequence data is accessible in the NCBI Sequence Read Archive under BioProject ID PRJNA278075.

Results

Across-shelf oxygen and nutrient distributions

Strong gradients in temperature and salinity were observed both vertically and horizontally across the northern Louisiana Shelf (Fig. 1), and also varied temporally at Sta. 6 likely due to water mass advection (Supporting Information Fig. S1). An intrusion of warm (> 30°C), low salinity (< 28) surface water was evident west of 90°W in the vicinity of the outflow of the Atchafalaya River and diminished along a westward gradient (Fig. 1a). Bottom waters were more saline (> 33; Fig. 1d), but remained warm (> 28°C) along the shallow shelf west of 90°W. Deeper waters to the east (Sta. 2 and Sta. 3) were cooler and more saline (Fig. 1d). The lowest oxygen concentrations during the late July-early August 2012 sampling period were observed west of 92°W, where bottom water concentrations ranged from 16 μmol kg^{-1} to 74 μmol kg^{-1} (Fig. 1e). Hypoxic conditions ([O_2] < 63 μmol kg^{-1}) were only seen at Sta. 6 and Sta. 8, with the lowest oxygen concentrations (16.4 μmol kg^{-1}) observed at Sta. 6 on 29th July. The oxygen distribution was consistent with data from monitoring cruises, which recorded hypoxic bottom waters over only 7480 km^2 of the Louisiana Shelf, the fourth smallest hypoxic zone measured since mapping commenced in 1985 (LUMCON 2012, http://www.gulfhypoxia.net/Research/Shelfwide%20Cruises/2012/, Accessed June 8th 2014). Reduced summertime hypoxia in 2012 was likely due to preceding drought conditions across the upper midwestern U.S.A., resulting in below average freshwater and nutrient discharge in spring (LUMCON 2012).

Low oxygen concentrations were associated with maximum nitrite concentrations (up to 4.6 μmol L^{-1}; Fig. 2a), consistent with an overall inverse relationship between nitrite and oxygen throughout the study area ($r^2 = 0.69$; $p < 0.05$; Fig. 2a). Nitrate concentrations fell in the range 0.1–11.4 μmol L^{-1} (median 0.5 μmol L^{-1}) and were weakly correlated with oxygen ($r^2 = 0.25$; $p < 0.05$), but not nitrite ($r^2 = 0.1$; $p > 0.05$) across all sites (data not shown). Indeed, maximum nitrate concentrations occurred at 120 m, at Sta. 3, the deepest and most oxygenated site in the study area. Ammonium concentrations across sampling sites ranged from below our detection limit (20 nmol L^{-1}) to 0.72 μmol L^{-1} and did not show a clear longitudinal trend nor a strong relationship to oxygen ($r^2 = 0.27$; $p < 0.05$; data not shown). However, at all sites, the highest ammonium concentrations were observed at the deepest sampling depths, with concentrations in the range 0.37–0.72 μmol L^{-1}.

Community taxonomic composition—16S rRNA genes

Analysis of 16S rRNA gene amplicons (median: 5005 per sample; Supporting Information Table S2) revealed a diverse microbial assemblage. Rarefaction at a minimum sequence depth ($n = 661$) did not identify consistent differences in alpha diversity among samples (Supporting Information Table S2), and NMDS clustering based on Bray Curtis distances did not clearly partition communities based on sample site (Fig. 3). However, the relative abundance of major taxonomic groups, notably the Thaumarchaeota, Euryarchaeota (Marine Group-II), and Cyanobacteria, varied substantially among sites. Marine Group-II, for example, represented 50% of all amplicons in the surface (2 m) sample from Sta. 4, but < 10% on average (all depths) at Sta. 1. In contrast, Sta. 1, located nearest the mouth of the Mississippi River, was enriched in *Synechococcus*, which constituted ~ 40% of amplicons at the three sampled depths, compared to an average of 12% at other sites. Time series sampling at 7 m and 15 m at Sta. 6 also revealed significant fluctuations in community structure over short (hours) timescales, likely due to water mass advection (Supporting Information Fig. S1).

Despite this variability, some community compositional trends were consistent across sites. Fitting environmental variables (oxygen, depth, pH, temperature, salinity, nitrate,

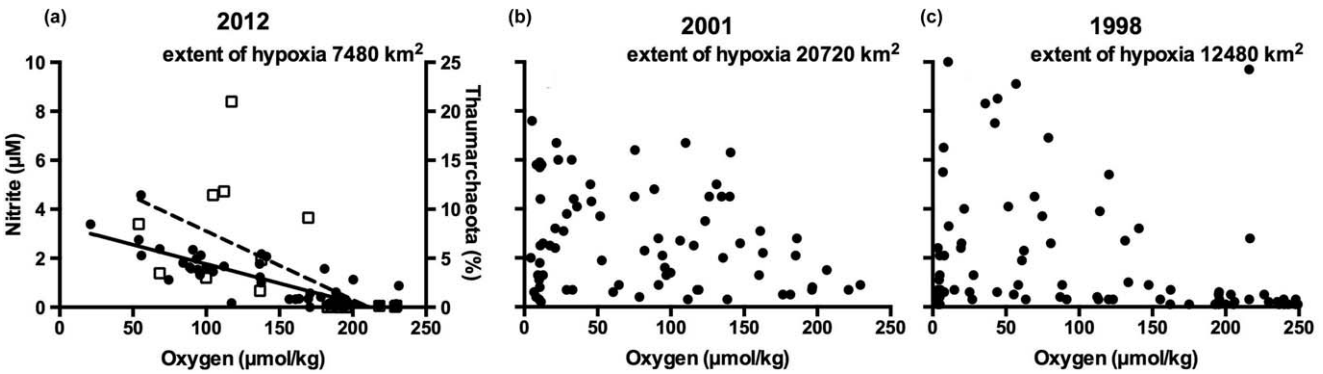

Fig. 2. Correlations between nitrite (μmol L^{-1}) and oxygen (μmol kg^{-1}) concentrations (black circles) from this study (July 2012; a, solid black line $r^2 = 0.69$, $p<0.05$), and from the NODC database for 2001 and 1998 (b and c), representing different extents of hypoxia. Panel a also shows Thaumarchaeota abundance (% of total 16S rRNA gene amplicons; open squares) with the dashed line representing the line of best fit ($r^2 = 0.41$; $p < 0.05$).

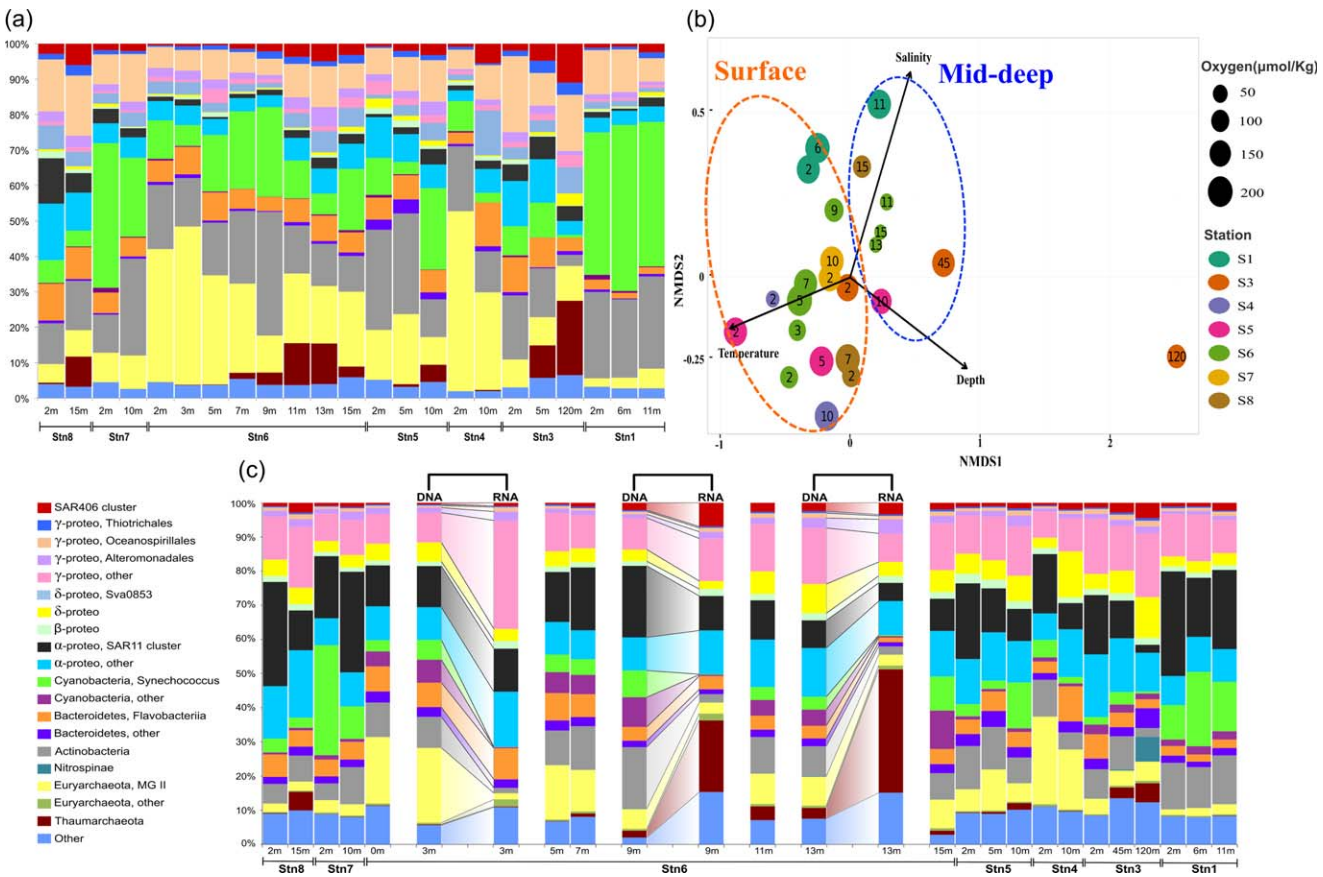

Fig. 3. Relative abundances of microbial taxa based on (a) 16S rRNA gene amplicons and (c) protein-coding gene sequences in metagenomes and metatranscriptomes. Metatranscriptome datasets (RNA, $n = 3$, Sta. 6) are connected to corresponding metagenome datasets (DNA). Panel b shows sample relatedness based on an NMDS ordination plot of 16S rRNA gene amplicon community structure with fitted environmental factors (depth, temperature, salinity; p value cutoff ≥ 0.001). Oxygen content at the sample site is represented by marker size. Numbers in bubbles are depths (m), with surface (< 10 m) and mid-deep (≥ 10 m) clusters circled, excluding the 120 m outlier. Note that circled clusters are not exclusive, as the surface set includes some 10 m samples.

nitrite, and ammonium) onto an NMDS ordination (Fig. 3b) revealed that oxygen concentration was not a driver of taxonomic composition ($r^2 = 0.04$, p value = 0.7). Consistent with results of Tolar et al. (2013), composition was instead correlated with depth ($r^2 = 0.90$, $p = 0.001$), temperature ($r^2 = 0.88$, $p = 0.001$), nitrate (r^2=0.79, $p = 0.005$), and salinity

($r^2 = 0.59$, $p = 0.001$). Notably, NMDS clustering revealed a general separation between surface (< 10 m) and mid-deep (≥ 10 m) communities, with the deepest sample, from 120 m at Sta. 3, as an outlier (Fig. 3b; Supporting Information Material).

Microorganisms involved in the two steps of nitrification showed contrasting distributions. Sequences affiliated with the ammonia-oxidizing Thaumarchaeota, predominantly the genus *Nitrosopumilus* (> 95% of Thaumarchaeota sequences), consistently increased in relative abundance with depth, peaking at 20% of total 16S amplicons at 120 m at Sta. 3. This depth-specific trend was driven by a moderate inverse correlation between relative Thaumarchaeota abundances and oxygen concentration (r^2=0.41; $p < 0.001$; Fig. 2a). NOB of the *Nitrospina* and *Nitrospira* were detected in amplicon pools from only two samples, from 45 m and 120 m at Sta. 3. NOB abundance peaked at 2.5% at 120 m, with *Nitrospina* (classified as Deltaproteobacteria in Fig. 3a, based on the Greengenes taxonomy), representing 92% of total NOB sequences. Low representation of NOBs across samples prevented a quantitative assessment of abundance relative to environmental conditions.

Taxonomic and functional gene trends—Meta-omic data

Estimates of taxonomic composition based on protein-coding genes and transcripts agreed broadly with results from the 16S rRNA gene data, notably supporting the depth-specific increase in Thaumarchaeota abundance (Fig. 3). Minor differences between data types included a proportionately higher representation of *Nitrospina* sequences (~ 7%) in the 120 m metagenome sample from Sta. 3 (compared to 2.3% in amplicon data) and an overall enrichment of Alphaproteobacteria of the SAR11 cluster in the meta-omic data compared to amplicon datasets. Such differences may be due to variation in the relative representation of taxa in 16S rRNA versus protein-coding gene databases, or biases inherent in the sequencing approaches.

The proportional abundances of taxonomic groups in the three metatranscriptome datasets varied markedly across depths (Fig. 3). Notably, the representation of Thaumarchaeota transcripts, identified based on database gene annotations, increased from less than 1% of identifiable protein-coding transcripts at 3 m to over 30% of the dataset at 13 m (Fig. 3), where Thaumarchaeota representation was over 10-fold higher than in the corresponding metagenome (DNA). In contrast, sequences matching diverse Gammaproteobacteria were overrepresented in RNA compared to DNA datasets at the surface compared to deeper depths, whereas groups such as the cyanobacteria, Euryarchaeota, and Actinobacteria were underrepresented in the transcript pool relative to the DNA pool across all depths. Representation of the ubiquitous SAR11 cluster of Alphaproteobacteria was relatively even in both RNA and DNA datasets (~ 10% on average), across all depths. These results indicate, not surprisingly, that relative representation in DNA datasets is a poor proxy for proportional contribution to community transcription.

The relative abundances of major functional gene categories varied between surface and mid-deep metagenomes, notably with processes of metabolism, including energy, carbohydrate and amino acid metabolism, significantly enriched at deeper depths, whereas surface depths were enriched in genes of genetic information processing (e.g., transcription, replication, and repair) and cellular communication (q-value < 0.05, GSEA; Supporting Information Table S3). Of the metabolic genes, those mediating nitrogen metabolism (KEGG ko00910) were also proportionately more abundant in deeper waters (Fig. 4), although this trend was not statistically supported (q-value > 0.05, GSEA).

Detected nitrogen metabolism genes and transcripts included those mediating nitrite production by both ammonia oxidation and nitrate reduction (Figs. 4 and 5). Notably, the ammonia monooxygenase gene *amoC* was detected in 18 of 23 samples at abundances from 6×10^{-5}% to 8×10^{-3}%, with a maximum at 120 m at Sta. 3, and *amoC* transcripts were also among the most abundant in Sta. 6 metatranscriptomes, increasing with depth from 0.009% at 3 m to 0.672% at 9 m and 1.009% at 13 m. The majority (> 75%) of *amoC* genes and transcripts were affiliated with Thaumarchaeota (Fig. 5). The *narG* gene, a marker for nitrite production by dissimilatory nitrate reduction, was detected in 22 of 23 samples at abundance ranging from 2.5×10^{-4}% to 9×10^{-3}%, with the maximum at 120 m at Sta. 3, consistent with an overall trend of increasing respiratory nitrate reductase genes in bottom waters (q-value < 0.05, GSEA; Fig. 4). As observed in other low-oxygen sites (Stewart et al. 2012; Yu et al. 2014), *narG* genes were affiliated with a diverse range of prokaryotes (data not shown). Compared to *amo* transcripts, NarG-encoding transcripts were at low abundances (0.001–0.004%) at Sta. 6 and did not exhibit clear depth-specific trends. In contrast to marker genes for nitrite production pathways, a marker gene for aerobic nitrite oxidation, *nxrB*, encoding the nitrite oxidoreductase beta subunit, was consistently low throughout the study area (< 0.0001%) and detected in only 5 of the 23 metagenomes. NxrB transcripts were not detected in the 3 m metatranscriptome from Sta. 6, and were at low abundance (0.001%) at both 9 m and 13 m, with all reads affiliated with *Nitrospina gracilis*.

Ammonia and nitrite oxidation rates

Ammonia oxidation rates ranged widely, from 9 nmol L^{-1} d^{-1} to 494 nmol L^{-1} d^{-1} across the Shelf (Fig. 5). Highest rates were observed in the hypoxic bottom waters (20 μmol O_2 kg^{-1}) of Sta. 6 on 29th July, and were associated with elevated nitrite concentrations (3.4 μmol L^{-1}; Fig. 5). Maximal rates observed here are higher than the typical maxima observed in other low oxygen regions (Lipschultz et al. 1990; Beman et al. 2012; Berg et al. 2014). However, these rates are significantly lower than those measured by the isotope

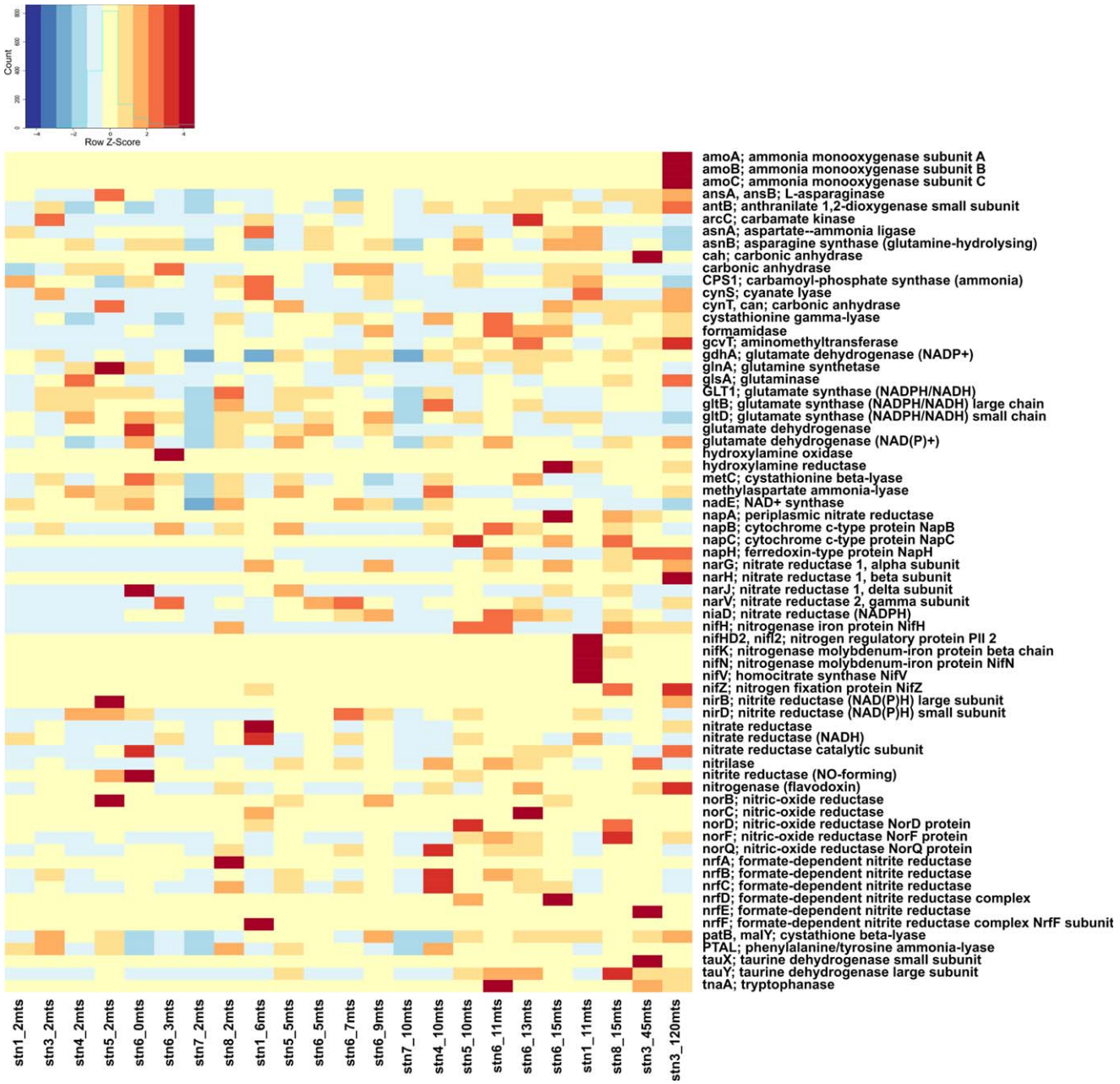

Fig. 4. Relative abundances of alphabetically sorted genes matching KEGG categories of Nitrogen Metabolism (ko00910). Station depths are arranged from surface (left) to mid-deep/deep (right). The color key indicates KEGG category abundance centered and scaled across stations (each value forced to have a mean of zero and standard deviation of 1), and expressed as a *Z*-score (standard deviations above or below the mean).

dilution method in the GoM in July 2008 under hypoxic conditions, where rates of nitrification up to 3.5 μmol L^{-1} d^{-1} were recorded (Carini et al. 2010). Although *amoC* sequences were detected in most metagenome samples, a clear correlation between ammonia oxidation rates and proportional *amoC* abundances was not observed (Fig. 5).

Nitrite oxidation rates spanned a similarly wide range, from 1 nmol L^{-1} d^{-1} to 411 nmol L^{-1} d^{-1} (Fig. 5). These rates showed no correlation with nitrite concentrations ($r^2 = 0.06$; $p > 0.05$), but were weakly positively correlated with ammonia oxidation rates (r^2 =0.39; $p > 0.05$). At most stations and depths, ammonia oxidation outpaced nitrite oxidation, by up to 30 times. The largest discrepancy between the two processes was seen in the bottom waters at Sta. 4 and Sta. 6 (Fig. 5). Station 2 was the only station where nitrite oxidation exceeded ammonia oxidation and where nitrite concentrations did not increase with depth (Fig. 5). Nitrite oxidation rates at Sta. 2 and Sta. 6 generally

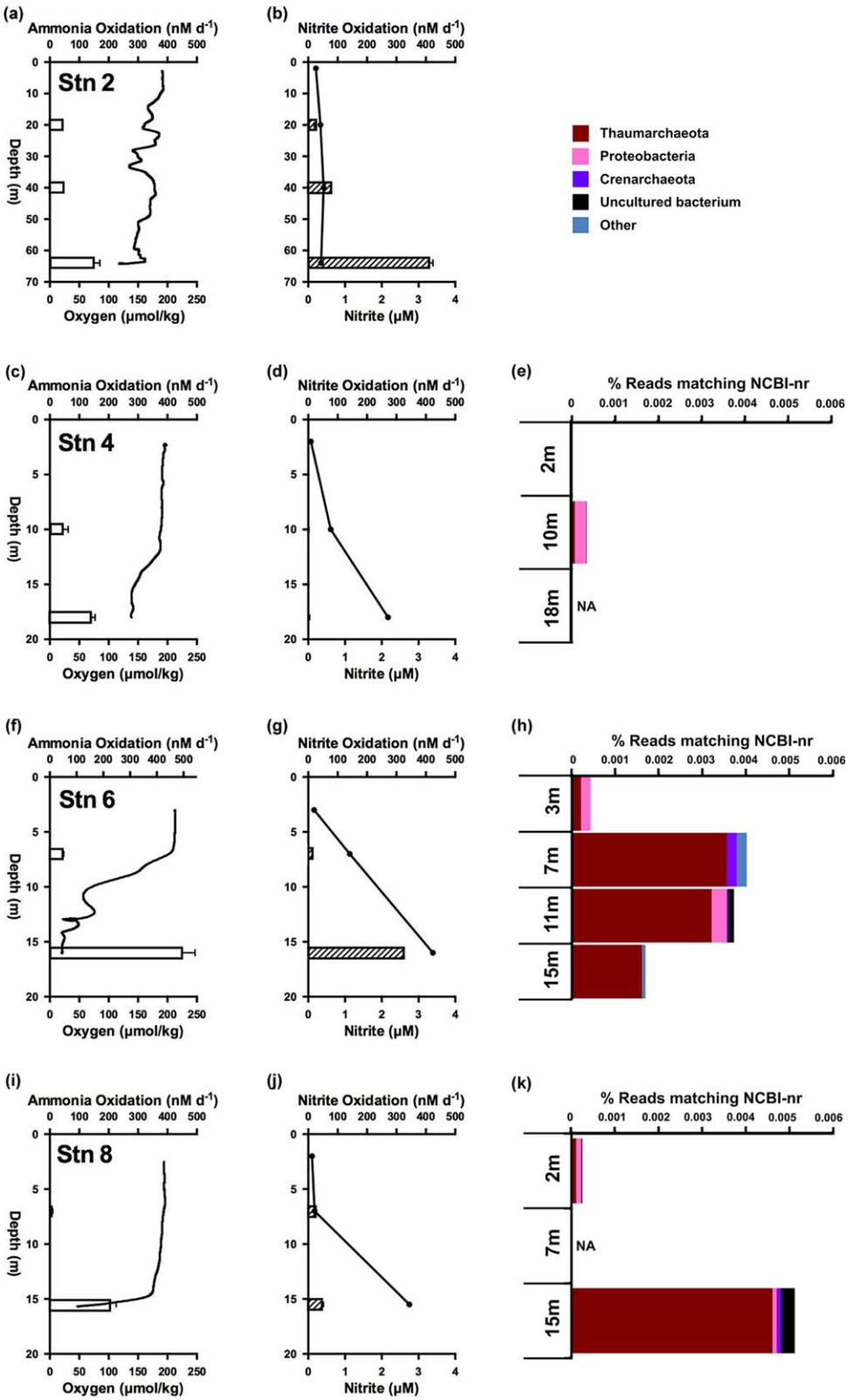

Fig. 5. Ammonia and nitrite oxidation rates and *amoC* gene abundances. Panels a, c, f, and i show ammonia oxidation rates (nmol L^{-1} d^{-1}; bars) and oxygen concentrations (μmol kg^{-1}). Panels b, d, g, and j show rates of nitrite oxidation (nmol L^{-1} d^{-1}; bars) and nitrite concentrations (μmol L^{-1}). Panels e, h, and k show the taxonomic representation and relative abundance of reads matching *amoC* in metagenomes. Error bars on ammonium and nitrite oxidation rates represent the standard error. Metagenome samples were not available for Sta. 2.

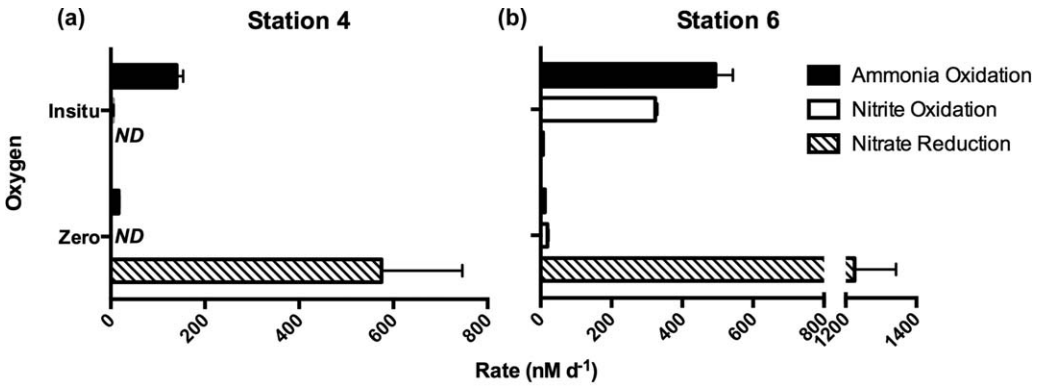

Fig. 6. Oxygen manipulation experiments from Sta. 4 (a) and Sta. 6 (b), showing nitrite production and consumption pathways (ammonia oxidation, nitrate reduction and nitrite oxidation), and their relative dominance over varying oxygen regimes (in situ (138 μmol kg^{-1} at Sta. 4 and 20 μmol kg^{-1} at Sta. 6) and anoxic conditions).

increased with depth and declining oxygen, whereas depth-specific increases were absent or less pronounced at Sta. 4 and Sta. 8. (The relative abundances of the nitrite oxidation gene *nxrB* in metagenome samples were zero or negligible and are not plotted in Fig. 5.)

Oxygen manipulation experiments

Oxygen manipulation experiments were conducted in the bottom waters of Sta. 4 and Sta. 6 to assess the oxygen sensitivity and relative roles of nitrite production and consumption processes in Shelf communities (Fig. 6). Under in situ oxygen concentrations (138 μmol kg^{-1} at Sta. 4, 20 μmol kg^{-1} at Sta. 6), nitrate reduction was only detected at Sta. 6, at a rate of 7 nmol L^{-1} d^{-1}. In contrast, ammonia and nitrite oxidation were detected at both stations at rates above 320 nmol L^{-1} d^{-1}, suggesting ammonia oxidation to be the dominant nitrite production pathway under in situ conditions. These patterns were reversed under anoxia. Ammonia and nitrite oxidation rates were below 20 nmol L^{-1} d^{-1} or not detected, whereas nitrate reduction rates were as high as 1185 nmol L^{-1} d^{-1}.

Discussion

Nitrite accumulation

Nitrite accumulated consistently under the low-oxygen conditions encountered over the Louisiana Shelf west of the Atchafalaya River in 2012. There was a strong inverse relationship between nitrite and oxygen, with nitrite reaching $\geq$1 μmol L^{-1} already at 150 μmol kg^{-1} oxygen, that is, substantially above the hypoxia threshold (Fig. 2). The majority of studies focusing on nutrient dynamics on the Shelf have presented dissolved inorganic nitrogen (DIN = nitrate + nitrite + ammonium), nitrate, and ammonium concentrations (e.g., Lohrenz et al. 1999; Rabalais et al. 2007; Quigg et al. 2011), but have not highlighted the distribution of nitrite. However, historical nitrite and oxygen data from 2001 and 1998, years representing high (20,720 km^2) and intermediate (12,480 km^2) levels of hypoxia compared to the 2012 minimum, suggest that nitrite accumulation occurs commonly under low oxygen conditions on the Louisiana Shelf, with nitrite concentrations up to 10 μmol L^{-1} observed under hypoxia (Fig. 2).

The persistent accumulation of nitrite to micromolar levels in marine waters is generally only observed under functional anoxia in OMZs. The primary nitrite maximum at the base of the photic zone is typically 0.01–0.5 μmol L^{-1} and rarely exceeds 1 μmol L^{-1} (Lomas and Lipschultz 2006 and ref. therein). A co-occurrence of micromolar nitrite and oxygen is observed occasionally in other environments, including diverse coastal ecosystems as a result of Thaumarchaeota ammonia-oxidizer blooms (Pitcher et al. 2011; Hollibaugh et al. 2014; Urakawa et al. 2014) and as transient occurrences due, for example, to mixing events, with a lifetime on the order of days (Mordy et al. 2010; De Brabandere et al. 2014). However, in other hypoxic shelf waters, nitrite typically remains below 1 μmol L^{-1} (Dale et al. 2011, 2014; Galán et al. 2014), with higher levels only reached, with nitrate reduction as the source, when oxygen approaches complete depletion (Naqvi et al. 2006; Füssel et al. 2012; Galán et al. 2014). The conditions on the Louisiana Shelf therefore appear unusual or even unique with respect to other hypoxic shelf systems, which raises questions about the underlying mechanisms and consequences of nitrite accumulation.

Our data suggest potential mechanisms controlling nitrite inventories on the Louisiana Shelf. Although oxygen concentrations below 16 μmol kg^{-1} were not observed during sampling, dissimilatory nitrate reduction could potentially contribute to the nitrite accumulation. Studies off Peru and over the Namibian shelf suggest that nitrate reduction exhibits varying sensitivity to oxygen, and can be observed up to oxygen concentrations of 25 μmol kg^{-1} (Kalvelage et al. 2011). Oxygen manipulation experiments at Sta. 4 and Sta. 6

suggested that nitrate reduction was not a significant source of nitrite (Fig. 6) and that ammonia oxidation was the dominant nitrite production pathway under in situ oxygen conditions. The lack of an inverse relationship between nitrite and nitrate concentrations further supports this conclusion. This is in line with Childs et al. (2002), who were unable to detect denitrification in the hypoxic bottom waters of the GoM. However, when identical experiments were carried out under anoxia, nitrate reduction became the dominant pathway for nitrite production (Fig. 6). If oxygen conditions were to drop further on the Shelf, which may be possible in years of more intense eutrophication and stratification, water column nitrate reduction could become a progressively larger contributor to Shelf nitrite accumulation. The potential for this shift is supported by the broad distribution of Nar-encoding genes in Shelf metagenomes (Fig. 4).

The important role for ammonia oxidation as a nitrite source under in situ oxygen conditions is further supported by the prevalence and activity of Thaumarchaeota across the Shelf. During July 2012, Thaumarchaeota represented up to 50% of total 16S rRNA gene sequences (Supporting Information Fig. S1; mean 5.9% across all samples) and were notably enriched in more oxygen-depleted layers, as were functional genes mediating ammonia oxidation (Figs. 3-5). In lower oxygen depths at Sta. 6 (9 m, 13 m), Thaumarchaeota genes in metatranscriptomes were $\sim$ 10-fold more abundant than those in metagenomes, with indicator genes for ammonia oxidation (*amo*) even more enriched in transcript datasets (up to 700-fold). Although the half-lives of AOA transcripts are unknown, and likely relatively short (Smith et al. 2014), the high representation of Thaumarchaeota in RNA datasets suggests an active ammonia oxidizer community. The observed Thaumarchaeota enrichment under lower oxygen (Fig. 2a) extends observations by Tolar et al. (2013) in the northern GoM during springtime prior to the development of hypoxia, at which time maximum Thaumarchaeota abundance coincided with the pelagic oxygen minimum (150 μmol kg^{-1}) at 200–400 m depth, while abundance over the Shelf was relatively low. The high abundance and activity of AOA under low oxygen is consistent with other studies of both hypoxic (Labrenz et al. 2010; Molina et al. 2010) and functionally anoxic systems (Lam et al. 2009; Beman et al. 2012; Stewart et al. 2012).

The large AOA population was likely supported by ammonium flux from the sediment, which peaks during summer hypoxia (Gardner et al. 1993; Rowe et al. 2002; Nunnally et al. 2013) with regeneration in the hypoxic bottom water, measured at rates of < 0.05 μmol L^{-1} h^{-1} (Gardner et al. 2009), as a possible additional source. The relatively low ammonium concentrations across Shelf bottom waters in July 2012 (0.37 μmol L^{-1} to 0.72 μmol L^{-1}), where AOA Thaumarchaeote abundance and nitrite concentrations were highest, are consistent with ammonia from the seafloor being efficiently oxidized to nitrite by AOA.

Consistently higher rates (up to 30-fold) of ammonia oxidation compared to nitrite oxidation, alongside an overall enrichment of *amoC* compared to *nxrB* genes and a relative absence of NOB 16S rRNA gene amplicons, suggest a strong decoupling between the two steps of nitrification, west of 90.7°W. This pattern was not observed at Sta. 2, the only site where nitrite oxidation outpaced ammonia oxidation and where nitrite accumulated to only moderate levels (< 0.5 μmol L^{-1}) (Fig. 5). The decoupling of ammonia from nitrite oxidation and consequent nitrite buildup observed at a subset of our stations contrasts with the results of Tolar et al. (2013), who found that the relative abundances of NOB in spring 2010, though only 0.4% on average, were correlated with those of Thaumarchaeota (slope = 0.05 NOB/Thaumarchaeota; $r^2 = 0.49$). These data were interpreted as evidence of coupling and a predicted efficient conversion of ammonium to nitrate. Here, using a deep-sequencing approach, rather than qPCR-based detection as in Tolar et al., we only detected NOB in two samples, which prohibited a detailed comparison of NOB and Thaumarchaeota distributions to better evaluate drivers of decoupling. Interpreted with the results of Tolar et al. (2013), our data suggest that the uncoupling of ammonia and nitrite oxidation over the Louisiana Shelf arises during the development of hypoxia and is hence potentially related to increased nutrient loading, oxygen depletion, or other factors associated with the spring to summer transition (e.g., temperature; *see* below).

Nitrite flux from the sediment is not likely to have contributed to the water column pool. Prior studies suggest that nitrite fluxes are small (–0.2 m^{-2} d^{-1} to 0.05 m^{-2} d^{-1}) and directed into the sediment under hypoxia, indicating that Shelf sediments are more likely a nitrite sink (Gardner et al. 1993; Rowe et al. 2002). Nitrite accumulation may also be linked to nitrite release by light-stressed phytoplankton (French et al. 1983; Collos 1998; Lomas and Glibert 1999; Lomas and Lipschultz 2006; Mackey et al. 2011). Although light levels were not measured in our study, no correlation between nitrite concentration and fluorescence was observed, suggesting phytoplankton release as an unlikely nitrite source during this study.

Together, this analysis suggests that nitrite accumulation in bottom waters of the shallow Louisiana Shelf is due primarily to a decoupling of ammonia and nitrite oxidation. Based on the offset between observed ammonia and nitrite oxidation rates, we approximate that it would take 13 to 20 days to yield the measured nitrite concentrations. These turnover times are intermediate in the relatively wide range of estimates for primary nitrite maxima (Santoro et al. 2013 and refs. therein). Beman et al. (2013) observed a decoupling between ammonia and nitrite oxidation in the ETNP and suggested this decoupling was generating the primary nitrite maximum and could do so in 1 to 5 days. In contrast, natural abundance dual isotopes of nitrite and nitrate determined

for the Arabian Sea enabled an estimate of nitrite turnover over a longer time period, suggesting that nitrite stocks in the region were derived primarily from ammonia oxidation and recycled every 33 to 178 days (Buchwald and Casciotti 2013). Shelf nitrite turnover rates estimated in this study are a first approximation and likely vary over interannual and seasonal gradients of primary production and riverine nutrient influx.

Factors driving decoupling in ammonia and nitrite oxidation

The decoupling between ammonia and nitrite oxidation could be linked to diverse factors, including oxygen concentration, substrate availability, and temperature.

Oxygen

The largest offsets between ammonia and nitrite oxidation rates (170 nmol L^{-1} d^{-1}; Fig. 5) occurred at Sta. 6 where oxygen concentration was lowest and rates of both processes were highest, with the exception of rates in bottom waters at Sta. 2. Under higher oxygen levels, the offset was reduced, and in the case of Sta. 2, nitrite oxidation exceeded ammonia oxidation and nitrite accumulated to only moderate levels (Fig. 5). While this trend and the inverse relationship between oxygen and nitrite concentrations (Fig. 2) suggest that oxygen limits nitrite oxidation, such limitation is inconsistent with an extensive literature showing efficient nitrite oxidation at considerably lower oxygen levels than found in this study, including systems without detectable oxygen where maximum nitrite oxidation rates higher than those observed here have been recorded (600 nmol L^{-1} d^{-1}, Lipschultz et al. 1990; 372 nmol L^{-1} d^{-1}, Füssel et al. 2012; 928 nmol L^{-1} d^{-1}, Kalvelage et al. 2013). Oxygen sensitivity experiments in OMZs over the Namibian Shelf and off Peru showed nitrite oxidation under low oxygen (< 1 μmol kg^{-1}) maintaining 36 to 59% of the activity measured at higher oxygen (> 10 μmol kg^{-1}) (Füssel et al. 2012; Kalvelage et al. 2013). This suggests that the K_m value for oxygen in NOB is at least as low as the value of 3.9 ± 0.6 μmol L^{-1} determined for oxygen respiration by the AOA *Nitrosopumilus maritimus* (Martens-Habbena et al. 2009). These observations are consistent with evidence for adaptation to low oxygen among marine NOBs of the *Nitrospina* and *Nitrospira* (Lücker et al. 2013). The nitrifying communities in the systems mentioned above appear similar to those in the GoM, with a dominance of AOAs (Beman et al. 2012; Stewart et al. 2012) and *Nitrospina* (Füssel et al. 2012; Beman et al. 2013; Levipan et al. 2014). These patterns suggest that oxygen is unlikely to be the primary factor limiting nitrite oxidation and therefore not directly driving the observed decoupling.

Substrate availability

Low oxygen levels instead may have contributed indirectly to the uncoupling of ammonia and nitrite oxidation. Ammonium efflux from Shelf sediments peaks during summer, seemingly due in part to increased oxygen limitation of benthic nitrification with the intensification of hypoxia (Nunnally et al. 2013). Ammonium concentrations in Shelf bottom waters were generally above the apparent K_m for AOA of 0.1 μmol L^{-1}, as determined from cultures of *Nitrosopumilus maritimus* and in a natural community in Puget Sound (Martens-Habbena et al. 2009: Horak et al. 2013), suggesting near-optimal growth conditions for AOA in the study area. In contrast, the optimal nitrite concentration for nitrite-oxidizing *Nitrospina watsonii* is 0.5–3 mmol L^{-1} (Spieck et al. 2014). Under optimal growth conditions, the doubling time for the AOA *N. maritimus* is $\sim$ 1 d (Martens-Habbena et al. 2009), whereas that of *Nitrospina* in culture is $\sim$ 0.5 d and $\geq$ 1 d for mixotrophic and lithotrophic growth, respectively (Watson and Waterbury 1971; Spieck et al. 2014). If these values are applicable to the GoM community, the above comparison predicts that NOB in the study area were nitrite-limited and that the AOA population would grow faster in response to increased substrate availability compared to nitrite-limited NOB, potentially resulting in the observed decoupling. Better constraints on in situ AOA and NOB growth rates over environmentally relevant temperature gradients are needed to test this hypothesis. This is complicated for NOB, as these bacteria may use substrates other than nitrite (Koch et al. 2014; Spieck et al. 2014).

Temperature

Studies of wastewater treatment systems suggest a role for temperature in decoupling ammonia and nitrite oxidation. Some treatment plants use a partial nitrification method by which ammonium is converted only to nitrite, before conversion to N_2 by either denitrification or anammox. This method requires conditions that favor ammonia oxidation over nitrite oxidation. Research to optimize this method shows that above 25°C nitrite oxidation and NOB growth slow, relative to ammonia oxidation and AOB growth (Balmelle et al. 1992; Hellinga et al. 1998). However, ammonia and nitrite oxidizers in wastewater facilities (primarily *Nitrosomonas* and *Nitrospira;* Egli et al. 2003) differ from those common in marine environments, notably AOA and *Nitrospina/Nitrospira*, and the sensitivity of natural AOA and NOB populations to seasonal variation in temperature is unknown. Louisiana Shelf waters experience wide temperature fluctuations with season (Xue et al. 2013), with summertime temperatures much warmer than those of winter and in off-shelf waters. The coupling of the two nitrification steps inferred by Tolar et al. (2013) in GoM waters was based on springtime samples collected when temperatures were $\leq$ 20°C. In contrast, Shelf bottom water was at 28–29.3°C during our study and NOB were only detected in deeper slope waters (45 m and 120 m) at Sta. 3, where temperatures were notably cooler (18–24°C). Furthermore, high temperature distinguishes our nitrite-rich stations from other hypoxic Shelf stations where nitrite concentrations remained < 1 μmol L^{-1} (Dale et al. 2011, 2014; Galán et al.

2014). These patterns, interpreted relative to results from wastewater systems, suggest that high summertime temperatures may contribute to a seasonal uncoupling of ammonia and nitrite oxidation on the Louisiana Shelf.

Potentially, salinity and photoinhibition could also play a role in the decoupling of ammonia and nitrite oxidation. Over large salinity gradients, both nitrification rates and the diversity and distribution of ammonia oxidizers have been shown to vary (Pakulski et al. 1995, 2000; Bernhard et al. 2005; Ward 2008). In our study, salinity varied relatively little, ranging from 35.8 to 32.8 in bottom waters, and from 27.4 to 32.3 in surface layers. The effect of such small gradients on nitrifier decoupling is unknown, but is likely to be irrelevant. Light has been shown to inhibit both ammonia and nitrite oxidizers (Ward et al. 1984; Ward 1987; Guerrero and Jones 1996). NOBs appear most sensitive, and this differential sensitivity has been suggested to contribute to the uncoupling associated with the formation of the oceanic primary nitrite maximum (Lomas and Lipschultz 2006). As all of our incubations were carried out in the dark, photoinhibition cannot be assessed from our experiments and cannot be ruled out as a driver of decoupling on the Louisiana Shelf.

Assembled together, our data reveal a Shelf ecosystem, subject to strong interlinking gradients in temperature, oxygen, nitrite and community structure. The first meta-omic data from the Louisiana Shelf identify a diverse microbial assemblage, with an important role for AOA, in agreement with prior work in the GoM (King et al. 2013; Tolar et al. 2013). Although AOA abundance did not correlate with ammonia oxidation rates, AOA contributed substantially to community transcription, occurred broadly across Shelf sites, and showed a general increase in abundance with depth and oxygen content, suggesting an important role for ammonia oxidation across Shelf oxygen gradients. In contrast to waters with lower oxygen content, nitrite production across the Shelf likely results primarily from ammonia oxidation, with nitrite accumulation driven by a decoupling of ammonia and nitrite oxidation rates, supported by low or undetectable numbers of NOB, and their functional genes. Decoupling likely stems from a combination of factors, with elevated bottom water temperature ($> 25°C$) and substrate limitation of nitrite oxidizers being the most likely contributors. High summertime temperatures may act to inhibit nitrite oxidizers but allow ammonia oxidizers to remain unchecked, permitting nitrite to accumulate. Substrate limitation may also be linked indirectly to both oxygen content and temperature.

These results indicate a complex nitrogen cycle on the Shelf, a region that remains surprisingly understudied from a community microbial perspective. The importance of nitrification, notably the ammonia oxidation step, to oxygen consumption in this region should not be overlooked in modeling studies. The ample pool of oxidized N available to the microbial community under low oxygen must continue to be monitored, and its production and consumption studied further with the potential expansion of low oxygen waters. Additional measurements of nitrite across diverse sites are needed to assess whether accumulation is a persistent feature in hypoxic systems, and to identify potential impacts on microbial N cycling pathways, algal speciation and new production estimates.

References

Balmelle, B., K. M. Nguyen, B. Capdeville, J. C. Cornier, and A. Deguin. 1992. Study of factors controlling nitrite build-up in biological process for water nitrification. Water Sci. Technol. **26**: 1017–1025.

Beman, J. M., J. Leilei Shih, and B. N. Popp. 2013. Nitrite oxidation in the upper water column and oxygen minimum zone of the eastern tropical North Pacific Ocean. ISME J. **7**: 2192–2205. doi:10.1038/ismej.2013.96

Beman, J. M., B. N. Popp, and S. E. Alford. 2012. Quantification of ammonia oxidation rates and ammonia-oxidizing archaea and bacteria at high resolution in the Gulf of California and eastern tropical North Pacific Ocean. Limnol. Oceanogr. **57**: 711–726. doi:10.4319/Lo.2012.57.3.0711

Benjamini, Y., and Y. Hochberg. 1995. Controlling the false discovery rate: A practical and powerful approach to multiple testing. J. R. Stat. Soc. Series B Methodol. **57**: 289–300. doi:10.2307/2346101

Berg, C., V. Vandieken, B. Thamdrup, and K. Jürgens. 2014. Significance of archaeal nitrification in hypoxic waters of the Baltic Sea. ISME J. doi:10.1038/ismej.2014.218

Bernhard, A. E., T. Donn, A. E. Giblin, and D. A. Stahl. 2005. Loss of diversity of ammonia-oxidizing bacteria correlates with increasing salinity in an estuary system. Environ. Microbiol. **7**: 1289–1297. doi:10.1111/j.1462-2920.2005.00808.x

Bianchi, T. S., S. F. DiMarco, J. H. Cowan, R. D. Hetland, P. Chapman, J. W. Day, and M. A. Allison. 2010. The science of hypoxia in the Northern Gulf of Mexico: A review. Sci. Total Environ. **408**:1471–1484. doi:10.1016/j.scitotenv.2009.11.047

Billen, G. 1975. Nitrification in the Scheldt Estuary (Belgium and the Netherlands). Estuar. Coast. Mar. Sci. **3**: 79–89. doi:10.1016/0302-3524(75)90007-9

Bouskill, N. J., D. Eveillard, G. O'Mullan, G. A. Jackson, and B. B. Ward. 2011. Seasonal and annual reoccurrence in betaproteobacterial ammonia-oxidizing bacterial population structure. Environ. Microbiol. **13**: 872–886. doi:10.1111/j.1462-2920.2010.02362.x

Braman, R. S., and S. A. Hendrix. 1989. Nanogram nitrite and nitrate determination in environmental and biological materials by vanadium (III) reduction with chemiluminescence detection. Anal. Chem. **61**: 2715–2718. doi:10.1021/ac00199a007

Brandhorst, W. 1958. Nitrite accumulation in the north-east tropical Pacific. Nature **182**: 679. doi:10.1038/182679a0

Buchwald, C., and K. L. Casciotti. 2013. Isotopic ratios of nitrite as tracers of the sources and age of oceanic nitrite. Nat. Geosci. **6**: 308–313. doi: 10.1038/ngeo1745

Caporaso, J. G., and others. 2010. QIIME allows analysis of high-throughput community sequencing data. Nat. Methods **7**: 335–336. doi:10.1038/nmeth.f.303

Carini, S. A., M. J. Mccarthy, and W. S. Gardner. 2010. An isotope dilution method to measure nitrification rates in the northern Gulf of Mexico and other eutrophic waters. Cont. Shelf Res. **30**: 1795–1801. doi:10.1016/j.csr.2010.08.001

Childs, C. R., N. N. Rabalais, R. E. Turner, and L. M. Proctor. 2002. Sediment denitrification in the Gulf of Mexico zone of hypoxia. Mar. Ecol. Prog. Ser. **240**: 285–290. doi: 10.3354/meps240285

Cline, J. D., and R. A. Richards. 1972. Oxygen deficient conditions and nitrate reduction in the eastern tropical North Pacific Ocean. Limnol. Oceanogr. **17**: 885–900. doi: 10.4319/lo.1972.17.6.0885

Collos, Y. 1998. Nitrate uptake, nitrite release and uptake, and new production estimates. Mar. Ecol. Prog. Ser. **171**: 293–301. doi:10.3354/meps171293

Dagg, M., J. Ammerman, R. W. Amon, W. Gardner, R. Green, and S. Lohrenz. 2007. A review of water column processes influencing hypoxia in the northern Gulf of Mexico. Estuaries Coasts **30**: 735–752. doi:10.1007/BF02841331

Dale, A. W., and others. 2011. Rates and regulation of nitrogen cycling in seasonally hypoxic sediments during winter (Boknis Eck, SW Baltic Sea): Sensitivity to environmental variables. Estuar. Coast. Shelf Sci. **95**: 14–28. doi:10.1016/j.ecss.2011.05.016

Dale, A. W., and others. 2014. Benthic nitrogen fluxes and fractionation of nitrate in the Mauritanian oxygen minimum zone (Eastern Tropical North Atlantic). Geochem. Cosmochim. Acta **134**: 234–256. doi:10.1016/j.gca.2014.02.026

Dalsgaard, T., B. Thamdrup, L. Farias, and N. P. Revsbech. 2012. Anammox and denitrification in the oxygen minimum zone of the eastern South Pacific. Limnol. Oceanogr. **57**: 1331–1346. doi:10.4319/Lo.2012.57.5.1331

De Brabandere, L., D. E. Canfield, T. Dalsgaard, G. E. Friederich, N. P. Revsbech, O. Ulloa, and B. Thamdrup. 2014. Vertical partitioning of nitrogen-loss processes across the oxic-anoxic interface of an oceanic oxygen minimum zone. Environ. Microbiol. **16**: 3041–3054. doi: 10.1111/1462-2920.12255

De Brabandere, L., B. Thamdrup, N. P. Revsbech, and R. Foadi. 2012. A critical assessment of the occurrence and extend of oxygen contamination during anaerobic incubations utilizing commercially available vials. J. Microbiol. Methods **88**: 147–154. doi:10.1016/j.mimet.2011.11.001

Diaz, R. J., and R. Rosenberg. 2008. Spreading dead zones and consequences for marine ecosystems. Science **321**: 926–929. doi:10.1126/science.1156401

Edgar, R. C. 2010. Search and clustering orders of magnitude faster than BLAST. Bioinformatics **26**: 2460–2461. doi: 10.1093/bioinformatics/btq461

Egli, K., C. Langer, H. R. Siegrist, A. J. B. Zehnder, M. Wagner, and J. R. van der Meer. 2003. Community analysis of ammonia and nitrite oxidizers during start-up of nitritation reactors. Appl. Environ. Microbiol. **69**: 3213–3222. doi:10.1128/AEM.69.6.3213-3222.2003

Francis, C. A., K. J. Roberts, J. M. Beman, A. E. Santoro, and B. B. Oakley. 2005. Ubiquity and diversity of ammonia-oxidizing archaea in water columns and sediments of the ocean. Proc. Natl. Acad. Sci. USA **102**: 14683–14688. doi: 10.1073/pnas.0506625102

French, D. P., M. J. Furnas, and T. J. Smayda. 1983. Diel changes in nitrite concentration in the chlorophyll maximum in the Gulf of Mexico. Deep-Sea Res. **30**: 707–722. doi:10.1016/0198-0149(83)90018-3

Füssel, J., P. Lam, G. Lavik, M. M. Jensen, M. Holtappels, M. Gunter, and M. M. M. Kuypers. 2012. Nitrite oxidation in the Namibian oxygen minimum zone. ISME J. **6**: 1200–1209. doi:10.1038/ismej.2011.178

Galán, A., J. Faúndez, B. Thamdrup, J. F. Santibáñez, and L. Farías. 2014. Temporal dynamics of nitrogen loss in the coastal upwelling ecosystem off central Chile: Evidence of autotrophic denitrification through sulfide oxidation. Limnol. Oceanogr. **59**: 1865–1878. doi:10.4319/lo.2014.59.6.1865

Ganesh, S., D. J. Parris, E. F. Delong, and F. J. Stewart. 2014. Metagenomic analysis of size-fractionated picoplankton in a marine oxygen minimum zone. ISME J. **8**: 187–211. doi: 10.1038/ismej.2013.144

García, H. E., and L. I. Gordon. 1992. Oxygen solubility in seawater – Better fitting equations. Limnol. Oceanogr. **37**: 1307–1312. doi:10.4319/lo.1992.37.6.1307

Gardner, W. S., E. E. Briones, E. C. Kaegi, and G. T. Rowe. 1993. Ammonium excretion by benthic invertebrates and sediment-water nitrogen flux in the Gulf of Mexico near the Mississippi river outflow. Estuaries **16**: 799–808. doi: 10.2307/1352438

Gardner, W. S., and others. 2009. Collection of intact sediment cores with overlying water to study nitrogen- and oxygen-dynamics in regions with seasonal hypoxia. Cont. Shelf Res. **29**: 2207–2213. doi:10.1016/j.csr.2009.08.012

Grasshoff, K., M. Ehrhardt, K. Kremling, and T. Almgren. 1983. Methods of seawater analysis, 2nd rev. and extended ed. Verlag Chemie.

Guerrero, M., and R. Jones. 1996. Photoinhibition of marine nitrifying bacetia. I. Wavelength dependent response. Mar. Ecol. Prog. Ser. **141**: 193–198. doi:10.3354/meps141183.

Hellinga, C., A. a. J. C. Schellen, J. W. Mulder, M. C. M. Van Loosdrecht, and J. J. Heijnen. 1998. The sharon process: An innovative method for nitrogen removal from ammonium-rich waste water. Water Sci. Technol. **37**: 135–142. doi:10.1016/S0273-1223(98)00281-9

Hollibaugh, J. T., S. M. Gifford, M. A. Moran, M. J. Ross, S. Sharma, and B. B. Tolar. 2014. Seasonal variation in the metatranscriptomes of a Thaumarchaeota population from SE USA coastal waters. ISME J. **8**: 685–698. doi: 10.1038/ismej.2013.171

Holmes, R. M., A. Aminot, R. Kérouel, B. A. Hooker, and B. J. Peterson. 1999. A simple and precise method for measuring ammonium in marine and freshwater ecosystems. Can. J. Fish. Aquat. Sci. **56**: 1801–1808. doi:10.1139/f99-128

Horak, R. E., and others. 2013. Ammonia oxidation kinetics and temperature sensitivity of a natural marine community dominated by Archaea. ISME J. **7**: 2023–2033. doi: 10.1038/ismej.2013.75

Kalvelage, T., and others. 2011. Oxygen sensitivity of anammox and coupled N-cycle processes in oxygen minimum zones. PLoS One **6**: e29299. doi:10.1371/journal.pone.0029299

Kalvelage, T., and others. 2013. Nitrogen cycling driven by organic matter export in the South Pacific oxygen minimum zone. Nat. Geosci **6**: 228–234. doi: 10.1038/ngeo1739

King, G. M., C. B. Smith, B. Tolar, and J. T. Hollibaugh. 2013. Analysis of composition and structure of coastal to mesopelagic bacterioplankton communities in the northern gulf of Mexico. Front. Microbiol. **3**: 438. doi:10.3389/fmicb.2012.00438

Koch, H., and others. 2014. Growth of nitrite-oxidizing bacteria by aerobic hydrogen oxidation. Science **345**: 1052–1054. doi:10.1126/science.1256985

Kozich, J. J., S. L. Westcott, N. T. Baxter, S. K. Highlander, and P. D. Schloss. 2013. Development of a dual-index sequencing strategy and curation pipeline for analyzing amplicon sequence data on the MiSeq Illumina sequencing platform. Appl. Environ. Microbiol. **79**: 5112–5120. doi:10.1128/AEM.01043-13

Labrenz, M., E. Sintes, F. Toetzke, A. Zumsteg, G. J. Herndl, M. Seidler, and K. Jürgens. 2010. Relevance of a crenarchaeotal subculster related to *Candidatus* Nitrosopumilus maritimus to ammonia oxidation in the suboxic zone of the central Baltic Sea. ISME J. **4**: 1496–1508. doi:10.1038/ismej.2010.78

Lam, P., and others. 2009. Revising the nitrogen cycle in the Peruvian oxygen minimum zone. Proc. Natl. Acad. Sci. USA **106**: 4752–4757. doi:10.1073/pnas.0812444106

Levipan, H. A., V. Molina, and C. Fernandez. 2014. *Nitrospina*-like bacteria are the main drivers of nitrite oxidation in the seasonal upwelling area of the Eastern South Pacific (Central Chile ~36°S). Enviorn. Microbiol. Reports **6**: 565–573. doi:10.1111/1758-2229.12158

Lipschultz, F., S. C. Wofsy, B. B. Ward, L. A. Codispoti, G. Friedrich, and J. W. Elkins. 1990. Bacterial transformations of inorganic nitrogen in the oxygen-deficient waters of the Eastern Tropical South Pacific Ocean. Deep-Sea Res. A **37**: 1513–1541. doi: 10.1016/0198-0149(90)90060-9

Lohrenz S. E., G. L. Fahnenstiel, D. G. Redalje, G. A. Lang, M. J. Dagg, T. E. Whitledge, and Q. Dortch. 1999. Nutrients, irradiance and mixing as factors regulating primary production in coastal water impacted by the Mississippi River plume. Cont. Shelf Res. **19**: 1113–1141. doi: 10.1016/S0278-4343(99)00012-6

Lomas M. W., and P. M. Glibert. 1999. Temperature regulation of nitrate uptake: A novel hypothesis about nitrate uptake and reduction in cool-water diatoms. Limnol. Oceanogr. **44**: 556–572. doi:10.4319/lo.1999.44.3.0556

Lomas, M. W., and F. Lipschultz. 2006. Forming the primary nitrite maximum: Nitrifiers or phytoplankton? Limnol. Oceanogr. **51**: 2453–2467. doi:10.4319/lo.2006.51.5.2453

Lücker, S., and others. 2010. A Nitrospira metagenome illuminates the physiology and evolution of globally important nitrite-oxidizing bacteria. Proc. Natl. Acad. Sci. USA **107**: 13479–13484. doi: 10.1073/pnas.1003860107

Lücker, S., B. Nowka, T. Rattei, E. Spieck, and H. Daims. 2013. The genome of nitrospina gracilis illuminates the metabolism and evolution of the major marine nitrite oxidizer. Front. Microbiol. **4**: 27. doi:10.3389/fmicb.2013.00027

Mackey, K. R. M., L. Bristow, D. R. Parks, M. A. Altabet, A. F. Post, and A. Paytan. 2011. The influence of light on nitrogen cycling and the primary nitrite maximum in a seasonally stratified sea. Prog. Oceanogr. **91**: 545–560. doi: 10.1016/j.pocean.2011.09.001

Magoc, T., and S. L. Salzberg. 2011. FLASH: Fast length adjustment of short reads to improve genome assemblies. Bioinformatics **27**: 2957–2963. doi:10.1093/bioinformatics/btr507

Malerba, M. E., S. R. Connolly, and K. Heimann. 2012. Nitrate-nitrite dynamics and phytoplankton growth: Formulation an experimental evaluation of a dynamic model. Limnol. Oceanogr. **57**: 1555–1571. doi:10.4319/lo.2012.57.5.1555

Martens-Habbena, W., P. M. Berube, H. Urakawa, J. R. De La Torre, and D. A. Stahl. 2009. Ammonia oxidation kinetics determine niche separation of nitrifying Archaea and Bacteria. Nature **461**: 976–979. doi:10.1038/nature08465

McCarthy, J. J., W. Kaplan, and J. L. Nevins. 1984. Chesapeake Bay nutrient and plankton dynamics. 2. Sources and sinks of nitrite. Limnol. Oceanogr. **29**: 84–98. doi: 10.4319/lo.1984.29.1.0084

McIlvin, M. R., and M. A. Altabet. 2005. Chemical conversion of nitrate and nitrite to nitrous oxide for nitrogen and oxygen isotopic analysis in freshwater and seawater. Anal. Chem. **77**: 5589–5595. doi:10.1021/ac050528s

Meyer, R. L., N Risgaard-Petersen, and D. E. Allen. 2005. Correlation between anammox activity and microscale distribution of nitrite in a subtropical mangrove sediment. Appl. Environ. Microbiol. **71**: 6142–6149. doi:10.1128/AEM.71.10.6142-6149.2005

Molina, V., L. Belmar, and O. Ulloa. 2010. High diversity of ammonia-oxidizing archaea in permanent and seasonal

oxygen-deficient waters of the eastern South Pacific. Environ. Microbiol. **12**: 2450–2465. doi:10.1111/j.1462-2920.2010.02218.x

Mordy, C.W., and others. 2010. Temporary uncoupling of the marine nitrogen cycle: Accumulation of nitrite on the Bering Sea shelf. Mar. Chem. **121**:157–166. doi:10.1016/j.marchem.2010.04.004

Mosier, A. C., and C. A. Francis. 2008. Relative abundance and diversity of ammonia-oxidizing archaea and bacteria in the San Francisco Bay estuary. Environ. Microbiol. **10**: 3002–3016. doi:10.1111/j.1462-2920.2008.01764.x

Naqvi, S. W. A., H. Naik, D. A. Jayakumar, M. S. Shailaja, and P. V. Narvekar. 2006. Seasonal oxygen deficiency over the western continental shelf of India, p. 195–224. *In* L. N. Neretin [ed.], Past and present water column anoxia. Springer. doi:10.1007/1-4020-4297-3_08

Nunnally, C. C., G. T. Rowe, D. C. O. Thornton, and A. Quigg. 2013. Sedimentary oxygen consumption and nutrient regeneration in the northern Gulf of Mexico hypoxic zone. J. Coast. Res. **63**: 84–96. doi:http://dx.doi.org/10.2112/SI63-008.1

Okasen, J., R. Kindt, P. Legendre, R. B. O'Hara. 2007. Vegan: Community ecology package version 1.8–6. Available from http://cran.r-project.org/ (Accessed on August 10 2014)

Olson, R. J. 1981. N-15 tracer studies of the primary nitrite maximum. J. Mar. Res. **39**: 203–226.

Pakulski, J. D., R. Benner, and R. M. W. Amon. 1995. Community metabolism and nutrient cycling in the Mississippi River plume: Evidence for intense nitrification at intermediate salinities. Mar. Ecol. Prog. Ser. **117**: 207–218. doi:10.3354/meps117207

Pakulski, J. D., and others 2000. Microbial metabolism and nutrient cycling in the Mississippi and Atchafalaya River Plumes. Estuar. Coast. Shelf Sci. **50**: 173–184. doi:10.1006/ecss.1999.0561

Pitcher, A., C. Wuchter, K. Siedenberg, S. Schouten, and J. S. Sinninghe Damsté. 2011. Crenarchaeol tracks winter blooms of ammonia-oxidizing Thaumarchaeota in the coastal North Sea. Limnol. Oceanogr. **56**: 2308–2318. doi:10.4319/lo.2011.56.62308

Quigg A., J. B. Sylvan, A. B. Gustafson, T. R. Fisher, R. L. Oliver, S. Tozzi, and J. W. Ammerman. 2011. Going west: Nutrient limitation of primary production in the Northern Gulf of Mexico and the importance of the Atchafalaya River. Aquat. Geochem. **17**: 519–544. doi:10.1007/s10498-011-9134-3

Rabalais, N. N., R. J. Díaz, L. A. Levin, R. E. Turner, D. Gilbert, and J. Zhang. 2010. Dynamics and distribution of natural and human-caused hypoxia. Biogeosciences **7**: 585–619. doi:10.5194/bg-7-585-2010

Rabalais, N. N., R. E. Turner, B. K. Sen Gupta, D. F. Boesch, P. Chapman, and M. C. Murrell. 2007. Hypoxia in the northern Gulf of Mexico: Does the science support the plan to reduce, mitigate, and control hypoxia? Estuaries Coasts **30**: 753–772. doi:10.1007/BF02841332

Rabalais, N. N., R. E. Turner, and W. J. Wiseman, Jr. 2001. Hypoxia in the Gulf of Mexico. J. Environ. Qual. **30**: 320–329. doi:10.2134/jeq2001.302320x

Rabalais, N. N., R. E. Turner, and W. J. Wiseman. 2002. Gulf of Mexico hypoxia, aka "The dead zone". Annu. Rev. Ecol. Syst. **33**: 235–263. doi:10.1146/annurev.ecolsys.33.010802.150513

Rowe, G. T., M. E. C. Kaegi, J. W. Morse, G. S. Boland, and E. G. E. Briones. 2002. Sediment community metabolism associated with continental shelf hypoxia, nothern Gulf of Mexico. Estuaries **25**: 1097–1106. doi:10.1007/BF02692207

Santoro, A. E., and others. 2013. Measurements of nitrite production in and around the primary nitrite maximum in the central California Current. Biogeosciences **10**: 7395–7410. doi:10.5194/bg-10-7395-2013

Schmidt, I., and others. 2003. New concepts of microbial treatment process for the nitrogen removal in wastewater. FEMS Microbiol. Rev. **27**: 481–492. doi:10.1016/S0168-6445(03)00039-1

Schmieder, R., Y. W. Lim, and R. Edwards. 2012. Identification and removal of ribosomal RNA sequences from metatranscriptomes. Bioinformatics **28**: 433–435. doi: 10.1093/bioinformatics/btr669

Schramm, A., D. De Beer., J. C. Van Den Heuvel, S. Ottengraf, and R. Amann. 1999. Microscale distribution of populations and activities of *Nitrosospira* and *Nitrospira* spp. Along a macroscale gradient in a nitrifying bioreactor: Quantification by in situ hybridization and the use of microsensors. Appl. Environ. Microbiol. **65**: 3690–3696.

Smith, J. M., K. L. Casciotti, F. P. Chavez, and C. A. Francis. 2014. Differential contributions of archaeal ammonia oxidizer ecotypes to nitrification in coastal surface waters. ISME J. **8**: 1704–1714. doi:10.1038/ismej.2014.11

Spieck, E. S. Keuter, T. Wenzel, E. Bock, and W. Ludwig. 2014 Characterization of a new marine nitrite oxidizing bacterium, *Nitrospina watsonii* sp. nov., a member of the newly proposed phylum "*Nitrospinae*". Syst. Appl. Microbiol. **37**: 170–176. doi:10.1016/j.syapm.2013.12.005

Stewart, F. J., O. Ulloa, and E. F. Delong. 2012. Microbial metatranscriptomics in a permanent marine oxygen minimum zone. Environ. Microbiol. **14**: 23–40. doi:10.1111/j.1462-2920.2010.02400.x

Thamdrup, B., T. Dalsgaard, and N. P. Revsbech. 2012. Widespread functional anoxia in the oxygen minimum zone of the eastern South Pacific. Deep-Sea Res. I **65**: 36–45. doi:10.1016/j.dsr.2012.03.001

Tian, L., S. A. Greenberg, S. W. Kong, J. Altschuler, I. S. Kohane, and P. J. Park. 2005. Discovering statistically significant pathways in expression profiling studies. Proc.

Natl. Acad. Sci. USA **102**: 13544–13549. doi: 10.1073/pnas.0506577102

Tolar, B. B., G. M. King, and J. T. Hollibaugh. 2013. An analysis of thaumarchaeota populations from the northern gulf of Mexico. Front. Microbiol. **4**: 72. doi:10.3389/fmicb.2013.00072

Turner, R. E., N. N. Rabalais, R. B. Alexander, G. McIssac, and R. W. Howarth. 2007 Characterization of nutrient, organic carbon, and sediment loads and concentrations from the Mississippi River into the northern Gulf of Mexico. Estuaries Coasts **30**: 773–790. doi:10.1007/BF02841333

Turner, R. E., N. N. Rabalais, and D. Justic. 2006. Predicting summer hypoxia in the northern Gulf of Mexico: Riverine N, P, and Si loading. Mar. Pollut. Bull. **52**: 139–148. doi: 10.1016/j.marpolbul.2005.08.012

Turner, R.E., N. N. Rabalais, and D. Justic. 2008. Gulf of Mexico hypoxia: Alternate states and a legacy. Environ. Sci. Technol. **42**: 2323–2327. doi:10.1021/es071617k

Turner, R. E., N. N. Rabalais, and D. Justic. 2012. Predicting summer hypoxia in the northern Gulf of Mexico: Redux. Mar. Pollut. Bull. **64**: 319–324. doi:10.1016/j.marpolbul.2011.11.008

Urakawa, H., W. Martens-Habbena, C. Huguet, J. R. de la Torre, A. E. Ingalls, A. H. Devol, and D. A. Stahl. 2014. Ammonia availability shapes the seasonal distribution and activity of archaeal and bacterial ammonia oxidizers in the Puget Sound Estuary. Limol. Oceanogr. **59**: 1321–1335. doi:10.4319/lo.2014.59.4.1321

Van Hulle, S. W. H., H. J. P. Vandeweyer, B. D. Meesschaert, P. A. Vanrolleghem, P. Dejans, and A. Dumoulin. 2010. Engineering aspects and practical application of autotrophic nitrogen removal from nitrogen rich streams. Chem. Eng. J. **162**: 1–20. doi:10.1016/j.cej.2010.05.037

Ward, B. B. 1987. Kinetic studies on ammonia and methane oxidation by *Nitrosococcus oceanus*. Arch. Microbiol. **147**: 126–133. doi:10.1007/BF00415273

Ward, B. B. 2008. Nitrification in marine systems, Chapter 5, p. 199–261. *In* D. G. Capone, D. A. Bronk, M. R. Mulholland, and E. J. Carpenter [eds.], Nitrogen in the marine environment, 2nd ed. Academic Press. doi:10.1016/B978-0-12-372522-6.00005-0

Ward, B. B., M. C. Talbot, and M. J. Perry. 1984. Contributions of phytoplankton and nitrifying bacteria to ammonium and nitrite dynamics in coastal water. Cont. Shelf Res. **3**: 383–398. doi:10.1016/0278-4343(84)90018-9

Watson, S. W., and J. B. Waterbury. 1971. Characteristics of two marine nitrite oxidizing bacteria, *Nitrospina gracilia nov. gen. nov. sp.* and *Nitrococcus mobilis nov. gen. nov. sp.* Arch. Mikrobiol **77**: 203–230. doi:10.1007/BF00408114

Xue, Z., R. He, K. Fennel, W. J. Cai, S. Lohrenz, and C. Hopkinson. 2013. Modeling ocean circulation and biogeochemical variability in the Gulf of Mexico. Biogeosciences **10**: 7219–7234. doi:10.5194/bg-10-7219-2013

Yu, Z., J. Yang, and L. Liu. 2014. Denitrifier community in the oxygen minimum zone of a subtropical deep reservoir. PLoS One **9**: e92055. doi:10.1371/journal.pone.0092055

Zhang, J., and others. 2010. Natural and human-induced hypoxia and consequences for coastal areas: Synthesis and future development. Biogeosciences **7**: 1443–1467. doi:10.5194/bg-7-1443-2010

Zhao, Y., H. Tang, and Y. Ye. 2012. RAPSearch2: A fast and memory-efficient protein similarity search tool for next-generation sequencing data. Bioinformatics **28**: 125–126. doi: 10.1093/bioinformatics/btr595

Acknowledgments

We thank the captain and crew of the *R/V Cape Hatteras* for help in sample collection, and Josh Parris and Sangita Ganesh for help in sample collection, preparation, and sequencing. We also thank Nancy Rabalais and other scientists who have contributed data to the NODC database for the northern Gulf of Mexico. This work was made possible by generous support from the National Science Foundation (1151698 to FJS), the Sloan Foundation (RC944 to FJS), the Danish National Research Foundation DNRF53, the Danish Council of Independent Research, and the European Research Council 'Oxygen' grant (267233; supporting LAB and BT).

Submitted 5 February 2015
Revised 28 April 2015, 3 June 2015
Accepted 8 June 2015

Associate editor: Caroline Slomp